Published in final edited form as:

Bone. 2017 February ; 95: 192–198. doi:10.1016/j.bone.2016.11.029.

Microdamage induced by *in vivo* Reference Point Indentation in mice is repaired by osteocyte-apoptosis mediated remodeling

Oran D. Kennedy[a,*], **Matin Lendhey**[a], **Peter Mauer**[b,c], **Anaya Philip**[b], **Jelena Basta-Pljakic**[b], and **Mitchell B. Schaffler**[b]

[a]New York University School of Medicine NY, United States [b]The City College of New York, NY [c]The Royal College of Surgeons in Ireland, Ireland

Abstract

Reference Point Indentation (RPI) is a technology that is designed to measure mechanical properties that relate to bone toughness, or its ability to resist crack growth, *in vivo*. Independent of the mechanical parameters generated by RPI, its ability to initiate and propagate microcracks in bone is itself an interesting issue. Microcracks have a crucial biological relevance in bone, are central to its ability to maintain homeostasis. In healthy tissues, a process of targeted remodeling routinely repairs microcracks in a process mediated by osteocyte apoptosis. However, in diseases such as osteoporosis this process becomes deficient and microcracks can accumulate. Small animal models such are crucial for the study of such diseases, but it is technically challenging to create microcracks in these animals without causing outright failure. Therefore we sought to use RPI as a focal microdamage placement tool, to introduce microcracks to mouse long bones and investigate whether the same pathway mediates their repair as that described in other microdamage systems. We first used SEM to confirm that microdamage is formed RPI in mouse bone. Then, since RPI is carried out transdermally, we sought to confirm that no periosteal response occurred at the indented region. We then used a pan-caspase inhibitor (QVD) to determine whether osteocyte apoptosis plays the same pivotal role in microdamage repair in this model, as has been demonstrated in others. In conclusion, we validated that the microdamage-apoptosis-remodeling pathway is maintained with this method of microdamage induction in mice. We show that RPI can be used as a reliable and reproducible microdamage placement tool in living mouse long bones without inducing a periosteal response. We also used a caspase inhibitor, to block osteocyte apoptosis and thus abrogate the remodeling response to microdamage. This demonstrates that the well described microdamage repair system, involving targeted remodeling mediated by osteocyte apoptosis, is conserved in this novel mouse model using an *in vivo* RPI loading system.

Keywords

RPI; Microcracks; Osteocyte; Apoptosis; Remodeling

[*]Corresponding author at: New York University School of Medicine, Orthopaedic Surgery, 301 East 17th Street, NY, NY 10003, United States. oran.kennedy@nyumc.org (O.D. Kennedy).

1. Introduction

Reference Point Indentation (RPI) is designed to measure mechanical properties of bone in order to assess the likelihood of fracture. Clinically, the successful identification of 'at-risk' patients with before fracture would allow for therapeutic intervention to reduce the risk of its occurrence [1,2]. Indeed some clinical studies have already demonstrated encouraging results using RPI in osteoporotic [3] and diabetic [4] cohorts. However, precisely what RPI parameters represent, in relation to traditional fracture toughness properties, remains unclear. Typical RPI parameters are First Cycle Indentation Distance (ID 1st), Total Indentation Distance (TID), Indentation Distance Increase (IDI), Creep Indentation Distance (CID), Mean Loading Slope (LS), Mean Unloading Slope (US) and Mean Energy Dissipation (ED). Preclinical studies in dogs showed that some of these parameters correlated well with mechanical properties such as modulus of toughness [5,6], which can be a useful index of a materials' ability to resist fracture. Other studies, mostly carried out in rodents, described a relatively poor correlation and high variability between and among standard measures [7,8]. The theoretical basis of RPI is that controlled application of force through an indenter probe at the bone surface creates a microscopic crack in the underlying tissue. This crack is then propagated by subsequent loading cycles at the same location. Diseased bone tissue possesses a diminished ability to resist crack initiation and propagation (*i.e.* has reduced fracture toughness) compared to healthy tissue. Thus the underlying concept of the RPI technique is that the output parameters it generates can act as a surrogate measurement for fracture toughness. Load and displacement data are continuously recorded during the test, and those parameters are calculated and used to index the overall structural integrity of the tissue.

Independent of these RPI mechanical parameters, the initiation and propagation of microcracks in bone tissue is an interesting issue in itself [9,10]. Microcracks have a crucial biological relevance in bone, and are central to maintaining its homeostasis [10,11]. Physiological levels of loading create microdamage on a regular basis, but healthy bone can remodel this damage efficiently. Aging, disease and drug-treatment can alter remodeling to such an extent that microdamage accumulates, and thus fracture risk is increased [11]. Osteocytes are central to this process due to their ability to detect microdamage [12]. They then orchestrate repair *via* osteocyte apoptosis, and modulation of osteoclastogenic signals such as RANKL and OPG in osteocytes adjacent to the apoptotic population [13–15]. More recently, the pannexin family of proteins was recently found to be a key player in this process. Panexxin 1 is a transmembrane protein that allows transport of small intracellular molecules to the extra-cellular space, and was found to play key role in the apoptotic signaling cascade in osteocytes *via* ATP release [16]. In those studies, the use of a transgenic mouse model was crucial, to causally link protein presence/activity to the functional behavior of osteocytes. However, the controlled introduction of microdamage into mouse long bones is challenging, time consuming and can be difficult to titrate. Typically microdamage is induced using *in vivo* fatigue (cyclic) loading of one of the long bones. In mice, the cortical thickness of the ulna is such that microcracks, even very early in their fatigue life, become large enough to result in rapid, outright fracture. Furthermore, while it is possible to estimate the location of the induced microdamage using this technique, based on

predictive stress analyses, it would be advantageous to have increased control of microdamage placement, and in a reduced timeframe.

Therefore we sought to use the BioDent *Hfc* system to test whether RPI can be used as a focal microdamage placement tool, and thus develop an alternative method of introducing microcracks to mouse long bones. We first developed a novel method to carry out reproducible RPI tests on living mouse bones. *In vivo* RPI parameters (ID-1st, CID, TID, IDI, LS, US and ED) have been successfully collected from mouse bones before [17], in a study of their variability in this species. Our method was slightly different and was specifically designed to confirm microcrack formation occurs beneath the indenter tip. Since RPI is carried out transdermally at the periosteal surface, we sought to determine whether it directly invokes a periosteal response in the indented region. A periosteal response under the point of application of force was reported in some early *in vivo* limb loading techniques, which used a 4-point bending technique along the diaphysis [18]. Finally, we sought to use a pan-caspase inhibitor to validate that the microdamage-apoptosis-remodeling pathway is maintained in this model. Thus we hypothesized that RPI can be used as a microdamage placement technique in mouse long bones, without evoking a periosteal response, and that a pan caspase inhibitor would inhibit the remodeling response to microdamage in this system.

2. Methods

2.1. Fixture design

Using SolidWorks software (Dassault Systèmes Solidworks Corp, MA, USA) we designed a device that would allow reproducible *in vivo* RPI testing of mouse tibiae using a BioDent *Hfc* research instrument (Active Life Scientific, SD). This was then fabricated in a modular fashion using 3D printing technology (ProJet 3510 SD, 3D Systems, SC, USA) and assembled prior to testing. The final design consisted of an upper platform on which the anesthetized mouse could be secured in a supine position. The lower platform, which was secured to the BioDent plate housed two adjustable upright posts to support sliding knee- and ankle-holders. The holders were allowed to translate, rotate and be fastened by screw lock mechanisms. The adjustable mid-span support post is an important design feature for this system. This feature provided a reaction force against the force applied during the test, to prevent the tibia bending during testing and could be raised/lowered to the desired height. Fig. 1A shows a representative schematic of an RPI test on a mouse tibia and Fig. 1B shows a photomicrograph of an *in vivo* RPI test being carried out *in situ*.

2.2. Microcrack validation using Reference Point Indentation (RPI)

We first carried out a validation study to confirm that microdamage occurs during RPI testing of mouse tibia using a BioDent device. The indenter probe assembly (BP2, Active Life Scientific, Santa Barbara, SD) consisted of: [1] outer reference probe (internal bore diameter 380 μm) that is inserted transdermally to rest on the bone surface, and [2] inner test probe, which is a cylindrical rod with a micro-machined conical tip (cone dimensions: 50 μm long, 50 μm base diameter, 2.5 μm tip-radius and 90° tip-angle) which indents the bone for a set number of cycles. A sub-group (n = 6) of tibia bones were tested *ex vivo* using the system described above. Based on previous studies, we selected an indentation site that was

immediately distal to the tibio-fibular junction (Fig. 1A), where the cortical thickness is greatest in this model. This site was located by measuring a fixed distance from the plantar surface of the foot. Before testing, the tibia was rotated externally by approximately 40°, so that the tibial crest was approximately parallel to the horizontal plane. The indentation site was shaved and cleaned and the probe was lowered on to the periosteal surface directly above the mid-span support post. Preconditioning cycling was carried out (4 cycles, 0.5 N, 2 Hz frequency) to account for the effects of periosteum/soft tissues and then 10 testing cycles were carried out (6 N at 2 Hz frequency). A representative image of the loading curves from one such test is shown in Fig. 2A.

2.3. Scanning Electron Microscopy

Scanning Electron Microscopy (SEM) was used to locate and assess the indentation sites on whole bone samples, and also to examine PMMA embedded undecalcified sections to assess the indentation profile, and any attendant microdamage. After testing, samples were fixed in 10% NBF, dehydrated in sequential alcohol solutions and incubated in physical vapor deposition chamber (Cressington Coating System 308R, USA) for gold (Au) coating. The deposition chamber was pressurized to 10-7 mbar to prevent the ionization of air. After the chamber was fully pressurized, evaporation supply or current source was used to deposit a 32 nm thick gold layer. A Cressington monitor was used to calculate layer thickness based on gold density. Samples were then imaged using a scanning electron microscope (Zeiss Inc., EVO40, USA) with secondary electron detector. The working distance was maintained at 8.5 mm, the sample plane was oriented perpendicular to the electron beam incidence, and a 9.5 kV accelerating voltage was employed with a 2.6 A operating current. Fig. 2B shows an indentation site on the periosteal surface of the tibia, taken from an intact whole bone sample. Fig. 2C shows an indentation in profile from a PMMA embedded section of the tibia, which was sequentially polished to expose the test site. This image also demonstrates a primary microcrack that has propagated from the indenter tip.

2.4. Experimental design

Under IACUC approval, young adult female C57B/6 mice (12–14 weeks old, Jackson Labs, ME) were acclimatized for one week prior to RPI testing. Two groups (SHAM and IND, n = 8/group) were used to test whether indentation caused a periosteal response, such as inflammatory cell infiltration, periosteum thickening or woven bone formation. To test the role of osteocyte apoptosis, the pan-caspase inhibitor QVD-OPh (quinolyl-valyl-Omethylaspartyl-[-2,6-difluorophenoxy]-methylketone, SM Biochemicals, Anaheim, CA) was used to prevent its occurrence after indentation. QVD operates *via* a carboxy terminal phenoxy group conjugated to the amino acids valine and aspartate to inhibit apoptosis, without cytotoxic side effects [19]. Three groups (CON, IND + VEH, IND + QVD n = 8/group) were used to determine whether microdamage induced using this method causes osteocyte apoptosis mediated remodeling. QVD has been shown in numerous studies from our laboratory not to have a demonstrable effect on osteocyte integrity or critical signaling in control rodents [13,15,16]. Beginning 2 h before indentation, one group of animals (IND + QVD) received QVD at 20 mg/kg/day by IP injection, while a second group (IND + VEH) received a corresponding dose of the DMSO vehicle. The CON group were anesthetized, positioned in the loading rig and exposed to probe placement, but indentation was not

carried out. Anesthesia was achieved using Avertin (20 mg/ml) delivered at a dosage of 125 mg/kg by intra-peritoneal injection. Buprenorphine was administered at a dosage of 0.1 mg/kg for analgesia. Animals were conscious and ambulatory within 20–30 min of the indent procedure. All animals were euthanized by CO2 asphyxiation after 14 days. The City College of New York Animal Care and Use Committee approved all procedures used in this study.

2.5. In vivo RPI

Anesthetized animals were secured on the upper platform, and the right tibia was secured between the knee and ankle fixtures and rotated externally by approximately 40° such that the tibial crest was parallel to the horizontal. The site was chosen as described above and the test was carried out in the same way. If a test was not successful due to slippage, or obviously erroneous loading curves, an additional test was carried out at a site 1 mm distal to the original. RPI data were continuously collected during testing, and then manufacturer software was used to calculate outcome parameters including ID 1st, CID TID, IDI, LS, US and ED. Data from all tests were pooled and descriptive statistics were calculated along with Coefficient or Variation (CoV) to assess reproducibility and reliability.

2.6. Periosteal response to RPI

To examine the periosteal response to RPI, tibiae were harvested after 14 days, fixed in 10% Neutral Buffered Formalin (NBF), decalcified in formic acid and then paraffin-embedded. Longitudinal serial-sections were taken in the sagittal plane of the tibia through the region where the indentation had been made. Toluidine Blue staining was used for morphological assessment of any woven bone response, and the periosteum thickness was measured as a surrogate for a periosteal response following indentation.

2.7. Remodeling and osteocyte apoptosis

Immediately after sacrifice, mice from the three groups used in the QVD study were re-positioned in the loading rig, and the limb was manipulated in the same way as for the original test. Then, an incision was made in the skin and a green tissue-marking dye (Shandon, Thermo Scientific, NY) was applied to the indention site to allow for its subsequent localization on histological sections. Tibiae were harvested as before, fixed in 10% NBF, decalcified, and paraffin-embedded. In this instance, serial cross-sections were made through the indent region, guided by the green tissue dye and three sections were taken every 50 μm. The first was unstained and used to confirm the presence of the green tissue dye; the second was stained with Toluidine Blue to identify morphological evidence of the indentation itself, and any associated resorption activity. The third section was used for IHC staining for cleaved caspase-3. For assessment of resorption activity, sections were rasterized and scanned at 5× magnification using bright-field microscopy and instances of resorption were identified morphologically.

For IHC sections were deparaffinized, re-hydrated, treated for 30 min with a methanol-NaOH solution for antigen retrieval (DeCal, Biogenex, San Ramon, CA), then blocked for a further 30 min (Rodent Block R, Biocare Medical, CA). Sections were then incubated overnight in a humidified chamber at 4 °C with a 1:100 dilution of rabbit antibody to

cleaved caspase-3 (#9661, Cell Signaling Technologies, Carpinteria, CA). Detection was performed using a goat *anti*-rabbit secondary antibody with a streptavidin-biotin conjugated system and developed with a DAB substrate chromogen system (Dako, Carpentaria, CA), after which the sections were dehydrated and cover-slipped using an aqueous mounting medium. Mouse growth plates processed in an identical manner were used as positive staining controls, and species-appropriate negative controls were also examined in each experiment. Osteocyte staining was assessed at 20×, using bright-field microscopy in a 1×1mm region of interest centered on the indentation site. The number of osteocytes that stained positive for caspase-3 were counted and calculated as a percentage of total osteocytes within the measurement region.

2.8. Statistical analysis

Statistical analyses were performed using the R software suite (Version 3.3.1, R Foundation, Austria). Initially, data were evaluated with the Kolmogorov-Smirnoff test to assess for normality of distribution. Coefficients of variation (CoV) were calculated across animals to assess variation of the indentation procedure in this model. Analysis of variance (ANOVA) testing was used to compare periosteal thickness and caspase-positive osteocyte count data, which were normally distributed. Kruskal-Wallis testing was used in lieu of ANOVA in the resorption cavity study, where the data were not normally distributed. All p-values < 0.05 were considered statistically significance.

3. Results

3.1. Microcrack validation and SEM

Our initial study qualitatively validated our ability to carry out *in vivo* RPI on the periosteal surface of the mouse tibia. Each sample had at least one successful indentation, as judged by an experienced user based on visual inspection of the loading curves. Two samples required three attempts, another required two and the remained were successfully indented on the first attempt. Indentations were located by SEM of whole bones in all but one of the samples, and had similar characteristics in all cases. In the plastic embedded sections the indentation profile, accompanied by evidence of at least one microcrack, was located in 50% of samples. In other cases, it is likely that the site was inadvertently removed by polishing.

3.2. In vivo RPI

All animals successfully underwent RPI testing on the anterior aspect of the right tibia, and returned to normal cage activity after testing. An experienced operator based the success of any given test on visual inspection of the loading curves. The variation in the calculated parameters between animals (CoV) ranged from 14 to 33% (Table 1). The least variable parameter was average slope of the loading curve (Avg LS), while the most variable was Indentation Distance Increase (IDI).

3.3. Periosteal response to RPI

Indentation loading did not evoke a periosteal woven bone response 14 days after indentation loading, nor was there any morphological evidence of focal soft tissue inflammation. Fig. 3A, B shows representative images from longitudinal sections taken

through the indentation site, and stained with Toluidine Blue. Our data showed a very slight non-significant increase in the periosteal thickness over the indentation site (Fig. 3C).

3.4. Remodeling and osteocyte apoptosis

Intracortical remodeling was activated below indentation sites in IND + VEH animals after 14 days (Fig. 4B) such remodeling sites were identified based on their morphological features and also by the fact that remodeling does not normally occur in these bones. Green tissue dye was also evident in many of the sections with resorption spaces, and can be seen in Fig. 4B, demonstrating spatial localization with the indentation site. These features were absent from CON and IND + QVD bones (Fig. 4A, C). Fig. 4D shows increased instances of intracortical resorption spaces in the IND + VEH group. IHC analyses showed strong positive staining for cleaved caspase-3 in osteocytes near the indentation-remodeling sites in the IND + VEH group (Fig. 5B), but not in CON or IND + QVD animals (Fig. 5A, C). Fig. 5B also shows resorption activity adjacent to caspase positive osteocytes near the periosteal surface of the tibia.

4. Discussion

The current studies are the first to show that a discrete intracortical remodeling response can be activated by placement of a microscopic damage focus in living mouse bone, and that this damage focus can be introduced acutely without evoking a woven bone response. Furthermore, the remodeling response to such damage is completely abrogated when apoptosis is inhibited using a pan-caspase inhibitor (QVD). These data suggest that the damage-remodeling pathway is functionally the same in this model compared to that seen with bone fatigue and microdamage *in vivo*. Our group and others have shown that the extent of microdamage induced through the microindentation process varies as a function of the indentation loads applied and the composition of the bone matrix [20,21]. Our novel approach provides the opportunity to titrate the size and extent of localized damage foci in future studies. Moreover, these results also represent an important advance in our ability to investigate targeted bone remodeling in both normal and genetically altered mouse bone, which should contribute greatly to our understanding of the *in situ* cellular and molecular controls of the damage-induced remodeling response.

Our SEM data showed that linear microcrack formation occurs at the indenter tip during testing in these mouse bones. While these cracks were not quantified here since our experiments were not designed to accurately measure microcrack characteristics, they were observed to be of the order of microcracks seen in other human and animal studies (10–30 μm in length). However, since linear microcracks play such an important role in this system, future studies will be required to evaluate their characteristics more definitively. Our laboratory previously showed that crack initiation at the indenter tip, and subsequent stepwise propagation with loading cycles, did not occur in the same way in human cadaveric bone [20]. This raises the important consideration that the RPI-induced damage mechanism may be different depending on bone type/age/disease-status or other constitutive tissue characteristics. The IDI parameter has been proposed as the most useful RPI output since it was shown to correlate well with fracture toughness in dogs [6]. In our studies, this was the

most variable parameter between animals, which is in agreement with other reports in the literature [17]. It is possible that a size effect of the tissue being tested influences this measurement, which would explain the observed variability in mouse bone, these and other tissue specific effects have been suggested by others [22].

Our initial *in vivo* indentation study was carried out to assess the extent of the periosteal response to the transdermal RPI test. In some of the early *in vivo* loading studies of rodent bone, four point bending tests were used to generate specific stress fields across the diaphysis. It was reported that the direct pressure created under the loading pads could cause an inflammatory periosteal response. This was partly why end-loading was developed, and is now the most widely used technique for this kind of experiment. In the normal adult mouse, intracortical osteoclast–mediated remodeling does not occur. Our group previously demonstrated that introduction of fatigue–induced microdamage to diaphyseal cortical bone can trigger targeted remodeling. We now demonstrate that indentation-induced microdamage also stimulates targeted-remodeling response in the same way in mouse bone. This allows microdamage placement to be achieved with improved spatial control. Furthermore, it may also offer more control over the extent of microdamage induced, and thus may allow for upper and lower limits for microcracks detection in bone to be defined. While 14 days may seem early for the initiation of the formation phase of the BMU, it may be that intracortical remodeling is relatively fast in mice compared to larger species. Although the tissue kinetics for intracortical remodeling in mice has not been thoroughly characterized, previous studies have reported similar findings [23]. Future studies using calcein labels for dynamic histomorphometry will be necessary to accurately characterize this response.

We also demonstrated that the osteoclastic resorption of indentation-induced microcracks in mouse bone is mediated by osteocyte apoptosis, which can be attenuated using QVD, a pan-caspase inhibitor. This demonstrates that this damage-dependent repair signaling system is functionally conserved in mice and this study can be compared with existing and previous data on this subject, which was largely carried out in other species. However, there may also be some differences in between this model and others. The rate of microcrack-induced apoptosis in the mouse may be relatively high compared to larger animals. We found evidence of widespread caspase-3 positive osteocytes near the indentation site 14 days after testing. Our previous studies used fatigue-induced damage in rats, and found a peak in caspase-3 positive osteocytes around 1 week. It is not possible to determine whether this is related to the type of testing, or the species used. Future studies of both will be useful in clarifying this issue.

The current study has certain limitations that should be acknowledged when considering these data. First, while the placement of microcracks *via* RPI is a convenient and reproducible way to induce microdamage, it is fundamentally different from the cyclically induced damage seen in human bone. The former is induced relatively quickly by direct force application at the periosteal surface, and the latter is an indirect consequence of fatigue loading of a complex and heterogeneous structure over a long time-period. Nonetheless, our data suggest that these methods produce sufficiently similar outcomes to allow comparisons between the two. Second, the precise characteristics of the RPI induced damage were not explored here, and these data will be crucial in order to fully characterize this kind of

damage from a mechanical and material perspective. However, the current study serves as a useful proof of concept, which paves the way for such a study in the future.

In conclusion, we show that RPI can be used as a reliable and reproducible microdamage placement technique in living mouse long bone without resulting in a periosteal response. We also used a pan caspase inhibitor QVD, to block osteocyte apoptosis and thus abrogate the remodeling response to microdamage in this system. This demonstrates that the well-described microdamage repair system, involving targeted remodeling mediated by osteocyte apoptosis, is conserved in this novel mouse model using an *in vivo* RPI loading system.

Acknowledgments

The authors are grateful to the Department of Orthopaedics at the NYU School of Medicine for funding support and to Damien Laudier for assistance with histological processing in this study. This work was supported by grants AR041210 and AR057139 from the National Institute of Arthritis and Musculoskeletal and Skin Diseases. The content is solely the responsibility of the authors and does not necessarily represent the official views of the National Institutes of Health.

References

1. Hansma P, Turner P, Drake B, et al. The bone diagnostic instrument II: indentation distance increase. Rev Sci Instrum. 2008; 79(6):064303. [PubMed: 18601422]
2. Hansma P, Yu H, Schultz D, et al. The tissue diagnostic instrument. Rev Sci Instrum. 2009; 80(5): 054303. [PubMed: 19485522]
3. Diez-Perez A, Guerri R, Nogues X, et al. Microindentation for in vivo measurement of bone tissue mechanical properties in humans. J Bone Miner Res. 2010; 25(8):1877–1885. [PubMed: 20200991]
4. Farr JN, Drake MT, Amin S, Melton LJ 3rd, McCready LK, Khosla S. In vivo assessment of bone quality in postmenopausal women with type 2 diabetes. J Bone Miner Res. 2014; 29(4):787–795. [PubMed: 24123088]
5. Aref M, Gallant MA, Organ JM, et al. In vivo reference point indentation reveals positive effects of raloxifene on mechanical properties following 6 months of treatment in skeletally mature beagle dogs. Bone. 2013; 56(2):449–453. [PubMed: 23871851]
6. Gallant MA, Brown DM, Organ JM, Allen MR, Burr DB. Reference-point indentation correlates with bone toughness assessed using whole-bone traditional mechanical testing. Bone. 2013; 53(1): 301–305. [PubMed: 23274349]
7. Carriero A, Bruse JL, Oldknow KJ, Millan JL, Farquharson C, Shefelbine SJ. Reference point indentation is not indicative of whole mouse bone measures of stress intensity fracture toughness. Bone. 2014; 69:174–179. [PubMed: 25280470]
8. Allen MRNC, Smith E, Brown DM, Organ JM. Variability of in vivo reference point indentation in skeletally mature inbred rats. J Biomech. 2014; 47(10):2504–2507. [PubMed: 24856912]
9. Burr D. Microdamage and bone strength. Osteoporos Int. 2003; 14(Suppl 5):S67–S72. [PubMed: 14504709]
10. Schaffier MB. Role of bone turnover in microdamage. Osteoporos Int. 2003; 14(Suppl 5):S73–S77. (discussion S7–80). [PubMed: 14504710]
11. Schaffier MB, Choi K, Milgrom C. Aging and matrix microdamage accumulation in human compact bone. Bone. 1995; 17(6):521–525. [PubMed: 8835305]
12. Verborgt O, Gibson GJ, Schaffier MB. Loss of osteocyte integrity in association with microdamage and bone remodeling after fatigue in vivo. J Bone Miner Res. 2000; 15(1):60–67. [PubMed: 10646115]
13. Cardoso L, Herman BC, Verborgt O, Laudier D, Majeska RJ, Schaffier MB. Osteocyte apoptosis controls activation of intracortical resorption in response to bone fatigue. J Bone Miner Res. 2009; 24(4):597–605. [PubMed: 19049324]

14. Kennedy OD, Herman BC, Laudier DM, Majeska RJ, Sun HB, Schaffier MB. Activation of resorption in fatigue-loaded bone involves both apoptosis and active pro-osteoclastogenic signaling by distinct osteocyte populations. Bone. 2012; 50(5):1115–1122. [PubMed: 22342796]
15. Kennedy OD, Laudier DM, Majeska RJ, Sun HB, Schaffier MB. Osteocyte apoptosis is required for production of osteoclastogenic signals following bone fatigue in vivo. Bone. 2014; 64:132–137. [PubMed: 24709687]
16. Cheung WY, Fritton JC, Morgan SA, et al. Pannexin-1 and P2X7-receptor are required for apoptotic osteocytes in fatigued bone to trigger RANKL production in neighboring bystander osteocytes. J Bone Miner Res. 2016; 31(4):890–899. [PubMed: 26553756]
17. Srisuwananukorn A, Allen MR, Brown DM, Wallace JM, Organ JM. In vivo reference point indentation measurement variability in skeletally mature inbred mice. Bonekey Rep. 2015; 4:712. [PubMed: 26131362]
18. Raab-Cullen DM, Akhter MP, Kimmel DB, Recker RR. Bone response to alternate-day mechanical loading of the rat tibia. J Bone Miner Res. 1994; 9(2):203–211. [PubMed: 8140933]
19. Caserta TM, Smith AN, Gultice AD, Reedy MA, Brown TL. Q-VD-OPh, a broad spectrum caspase inhibitor with potent antiapoptotic properties. Apoptosis. 2003; 8(4):345–352. [PubMed: 12815277]
20. Beutel BG, Kennedy OD. Characterization of damage mechanisms associated with reference point indentation in human bone. Bone. 2015; 75:1–7. [PubMed: 25659950]
21. Setters A, Jasiuk I. Towards a standardized reference point indentation testing procedure. J Mech Behav Biomed Mater. 2014; 34:57–65. [PubMed: 24556325]
22. Rasoulian R, Raeisi Najafi A, Chittenden M, Jasiuk I. Reference point indentation study of age-related changes in porcine femoral cortical bone. J Biomech. 2013; 46(10):1689–1696. [PubMed: 23676290]
23. Li CY, Jepsen KJ, Majeska RJ, et al. Mice lacking cathepsin K maintain bone remodeling but develop bone fragility despite high bone mass. J Bone Miner Res. 2006; 21(6):865–875. [PubMed: 16753017]

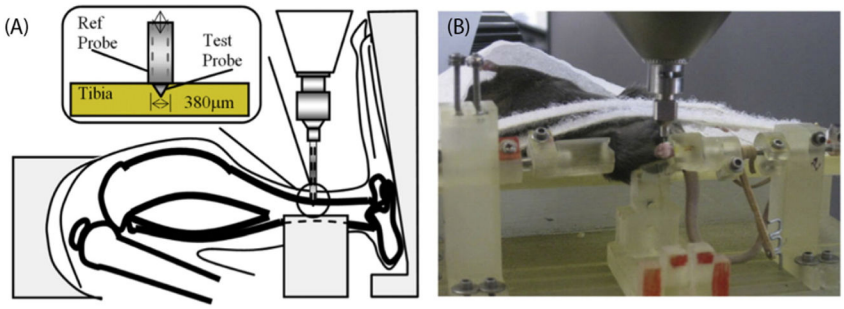

Fig. 1.

In vivo RPI loading of mouse tibia. (A) Schematic representation of indentation location and dimension of probe (Inset). (B) Photograph of custom designed, 3D printed fixture device with anesthetized mouse *in situ*.

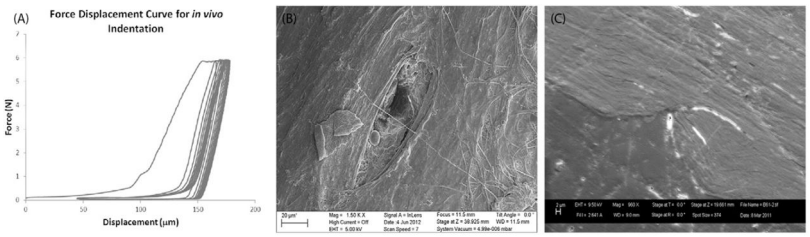

Fig. 2.

In vivo RPI induced microdamage validation. (A) Representative loading curves from *in vivo* loading of mouse tibia, showing successfully completed testing protocol with no slippage. (B) SEM photomicrograph of indentation site on periosteal surface of mouse tibia. (C) Representative photomicrograph of indentation profile in PMMA embedded polished section of tibia.

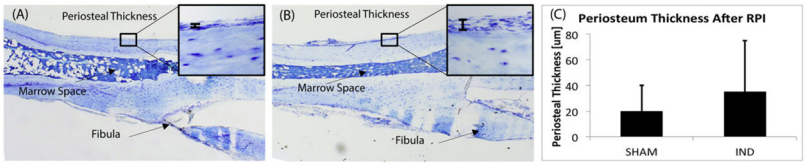

Fig. 3.

Periosteal response to *in vivo* RPI loading. Representative Toluidine Blue stained longitudinal sections of the mouse tibia centered at the indentation site, from (A) control and (B) indented tibiae, with high magnification image of the periosteum shown in each (inset). (C) Periosteal thickness data showing a slight non-significant increase 14 days after loading.

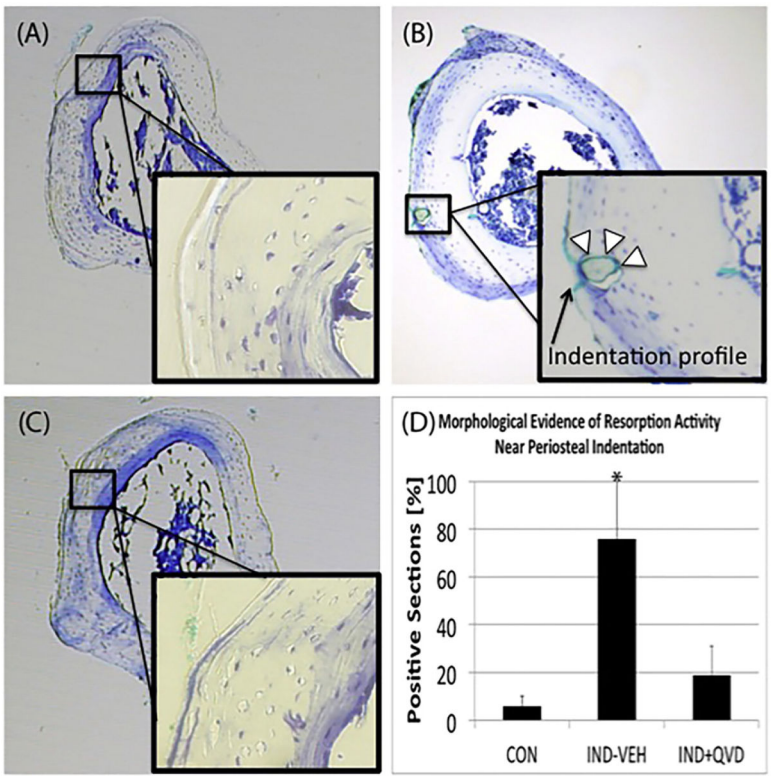

Fig. 4.

Intracortical remodeling response to *in vivo* RPI loading. Representative Toluidine Blue stained cross-sections of paraffin embedded mouse tibia, at 5× magnification showing (A, C) the absence of remodeling and in CON and IND + QVD groups (inset: cortex beneath indent, no evidence of remodeling) and (B) evidence of intracortical resorption activity in the IND + VEH group (inset: cortex beneath indentation showing an example of an active remodeling space adjacent to the indentation profile). (D) Shows data of instance of resorption in samples from all three groups.

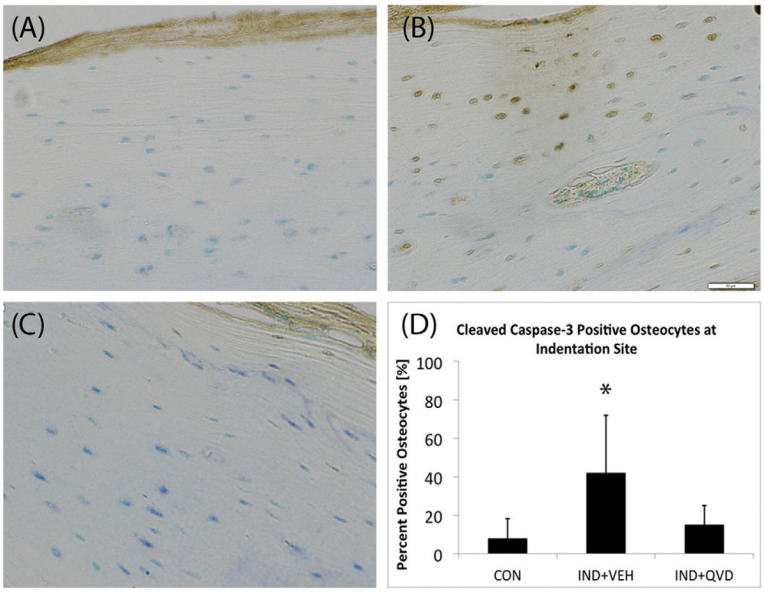

Fig. 5.

Role of osteocyte apoptosis in response to *in vivo* RPI loading. Representative IHC stained cross-sections of paraffin embedded mouse tibia, at 20× magnification showing (A, C) the absence of positively stained osteocytes in CON and IND + QVD groups and (B) clear evidence of positively stained osteocytes, morphological evidence of co-located intracortical resorption activity, in the IND + VEH group. (D) Shows data of percentage of positively stained osteocytes in samples from all three groups.

Table 1

Reference point indentation parameters from *in vivo* loading in tibiae of mice.

	First cycle indentation distance ID 1st (μm)	First cycle creep indentation distance CID (μm)	Creep indentation distance TID (μm)	Indentation distance increase IDI (μm)	Average energy dissipated Avg ED (μJ)	Average loading slope avg LS (N/μm)	Average unloading slope Avg US (N/μm)
Mean	47.3	6.9	62.4	14.1	49.9	0.34	0.82
Standard deviation	12.5	2.17	18.7	4.6	11.3	0.05	0.14
Coefficient of variation (%)	26.55	28.8	30.1	33.1	22.7	14.6	17.1